

# CrystEngComm

Accepted Manuscript



This is an *Accepted Manuscript*, which has been through the Royal Society of Chemistry peer review process and has been accepted for publication.

*Accepted Manuscripts* are published online shortly after acceptance, before technical editing, formatting and proof reading. Using this free service, authors can make their results available to the community, in citable form, before we publish the edited article. We will replace this *Accepted Manuscript* with the edited and formatted *Advance Article* as soon as it is available.

You can find more information about *Accepted Manuscripts* in the [Information for Authors](#).

Please note that technical editing may introduce minor changes to the text and/or graphics, which may alter content. The journal's standard [Terms & Conditions](#) and the [Ethical guidelines](#) still apply. In no event shall the Royal Society of Chemistry be held responsible for any errors or omissions in this *Accepted Manuscript* or any consequences arising from the use of any information it contains.

## ARTICLE

# Crystal structure analyses facilitate understanding of synthetic protocols in the preparation of 6,6'-dibromo substituted BINOL compounds

Cite this: DOI: 10.1039/x0xx00000x

Received 00th January 2012,  
Accepted 00th January 2012

DOI: 10.1039/x0xx00000x

www.rsc.org/

Marco Agnes,<sup>a,b</sup> Alessandro Sorrenti,<sup>a</sup> Dario Pasini,<sup>b</sup> Klaus Wurst<sup>c</sup> and David B. Amabilino<sup>a</sup>

A combination of crystallographic and spectroscopic techniques has been used in order to address thorough purification protocols for a series of atropoisomeric 1,1'-binaphthalene-2,2'-diol (BINOL) derivatives, to be used as building blocks for chiral nanoscale constructs. The compounds were obtained following an initial electrophilic aromatic bromination reaction at the 6,6' positions of BINOL, which was used either in racemic or enantiopure form. The presence of regioisomeric compounds, in which bromine atoms are located at different positions of the naphthalene skeletons, could be hinted at using classical spectroscopies (<sup>1</sup>H NMR and IR), and fully confirmed by single crystal X-ray analysis of the solids formed during crystal growth of the crude products, where solid solutions are identified in part thanks to the presence of bromine that is a relatively heavy atom. If purification by recrystallization in suitable solvents is not performed, further chemical elaboration by means of alkylation on the 2,2'-phenolic positions produce compounds in which the regioisomeric impurities are still present. The set of five X-ray structures highlights interesting packing features, extremely useful for the crystal engineering of nanostructures integrating these axially-chiral building blocks.

## Introduction

The translation of molecular chirality into supramolecular and nanoscale chirality have been the subject of intense research activity in recent years, and ordered chiral nanostructures have demonstrated potential for a number of bulk materials applications.<sup>1</sup> Substituted 1,1'-binaphthyl derivatives are a versatile class of compounds – chiral thanks to atropoisomerism because of hindered rotation around the bond linking the naphthyl groups – which have found applications in many different areas of chemistry.<sup>2</sup> Their chirality is a result of the angle between the aromatic rings caused by steric interactions and the restricted rotation around naphthalene-naphthalene bond mean that the enantiomers can be isolated in certain cases. The rigid structure and the C<sub>2</sub> symmetry of the binaphthyl skeleton are key factors in the efficient transfer of the chiral information. As a consequence of the favourable properties, these synthons have become attractive molecular modules in fields as diverse as asymmetric catalysis,<sup>3</sup> chiral supramolecular recognition<sup>4</sup> and crystal engineering.<sup>5</sup> Recent applications as building blocks for polymers,<sup>6</sup> and for chiroptical sensing have also emerged.<sup>7</sup> Perhaps the most common derivative, amongst

the class of substituted 1,1'-binaphthyl derivatives, is 2,2'-dihydroxy-1,1'-binaphthyl (**1**, Fig. 1), often referred as BINOL. Its basic skeleton can be conveniently functionalized in various positions; the most frequent ones are the 4,4' and 6,6' positions, but access to the 3,3'-positions is also well documented.<sup>2d,e</sup>

The functionalization in the 6,6' positions is most frequently achieved by means of an electrophilic bromination on the naphthalene rings. A plethora of synthetic opportunities, such as arylation and vinylation reactions via Stille or Suzuki-type couplings, has then been utilized to substitute the bromine atoms with specific functionalities.<sup>2d,2e,6</sup>

During the course of a continuing project dealing with the use of BINOL-based building blocks for functional nanostructures,<sup>8</sup> we turned our attention to 6,6'-disubstituted BINOL derivatives. In this paper, we report five novel crystal structures for a series of 6,6'-disubstituted BINOL derivatives, either in their racemic or enantiopure form. We describe how a combination of crystallographic and spectroscopic techniques have been used in a synergic way in order to identify minor amounts of impurities, and thus to set up thorough purification protocols to be used in the synthesis of these popular BINOL-based synthons. The results are obtained after a bromination of

the parent compound, and the identification of the impurities has been achieved thanks to the presence of bromine that is a

heavy atom easily identifiable by X-ray crystallography.

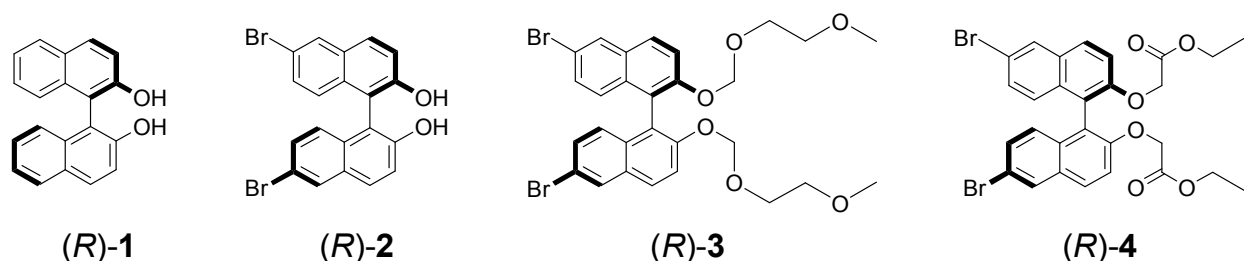


Fig. 1 Chemical structures of the compounds used in this study. Only (*R*) enantiomers are shown.

## Results and Discussion

**Synthesis, NMR Characterization and Purification Procedures.** The compounds described in this paper are shown in Fig. 1. They were synthesized using protocols described in the literature, or with minor modifications with respect to the reported procedures. The reactions were carried out on either racemic (*RS*)-**1** or enantiopure (*R*)-**1**, both commercially available compounds.

Compound **2** was prepared by electrophilic bromination of compound **1**.<sup>9</sup> Derivatization at the 2,2' phenolic positions was conducted in two different ways, under reaction conditions already established as non racemizing: a) protection with methoxyethoxymethyl (MEM) chloride to give compound **3**<sup>10</sup> and b) alkylation in mild basic conditions ( $\text{Cs}_2\text{CO}_3$ , DMF)<sup>11</sup> to get the diester compound **4**.

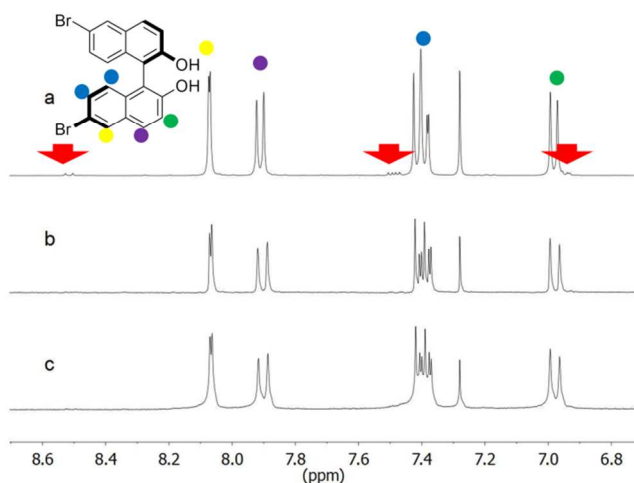


Fig. 2  $^1\text{H}$ -NMR spectra of (*R*)-**2** before (a) and after crystallization from different mixtures of solvents:  $\text{CH}_2\text{Cl}_2/\text{cyclohexane}$  (b) and toluene/*n*-hexane (c). The red arrows indicate the impurity.

The bromination step to give **2** has been reported to date to be nearly quantitative and regioselective for the 6,6'-positions as a consequence of the strong electron donating character of the OH groups in the 2,2'-positions.<sup>9,††</sup>

However, the  $^1\text{H}$ -NMR spectra of either enantiopure or racemic **2** after workup of the reaction showed some impurities in the aromatic region (Fig. 2a and Fig. S1). The impurities could not be readily attributed to a specific organic compound; the few small peaks not covered by other resonance signals (a doublet at 8.52 ppm, a multiplet at 7.49 ppm and a doublet at 6.93 ppm) hinted at a regioisomer in which the bromine atoms are placed at different positions on the two naphthalene units.

Impurities could be estimated to be around 10-12% of the product, and could not be removed by column chromatography. Complete purification of **2** (see NMRs Fig. 2b and 2c and Fig. S1) was achieved following standard crystallization protocols, screening different mixtures of solvents and evaluating the purity of the products after crystallization using  $^1\text{H}$  NMR spectroscopy. All the signals related to the impurities disappeared in the spectra taken after the crystallization from the solvents specified in Table 1 (entries 1-3 for compounds **2**). These crystallization solvent combinations can be therefore considered adequate for the purification. This compound, and the other chiral ones in this series, was characterised by circular dichroism spectroscopy that shows the expected exciton chirality for the enantiomer used in the synthesis (see ESI).

IR spectroscopy was also informative and supported the presence of impurities in the initially isolated material (Fig. S2). The peak at  $734\text{ cm}^{-1}$  in the spectrum of (*R*)-**2** immediately after the work up could correspond to stretching frequencies of C-Br bonds (usually in the region between  $730$  and  $750\text{ cm}^{-1}$ ) in different halogenated impurities. This data could also be consistent with a dibromosubstituted BINOL in which the two bromine atoms are at different positions of the naphthalene units. After the purification by crystallization from the appropriate mixture of solvents (Table 1), the peak at  $734\text{ cm}^{-1}$  is no longer present (Fig. S2, bottom). The absence of this peak demonstrates that unsymmetrically halogenated products have been removed successfully in this crystallisation; for comparison, the C-Br bond in the monohalogenated (symmetrical) pure product **2** stretches at  $670\text{ cm}^{-1}$ .

When regioisomerically contaminated samples of **2** were brought to the following synthetic steps without prior purification by crystallization, further purification of **3** or **4** by crystallization was not possible, and solid solutions of the different regioisomers were found in the X-ray crystal structure analysis (*vide infra*). On the other hand, regioisomerically pure

samples of compound **2** were able to generate, after chemical modifications, regioisomerically pure samples of **3** and **4**.

**Table 1** Solvent combinations used in the crystallization of compounds **2–4**.

Entry	Compound	Mixture of solvents <sup>a</sup>	Outcome <sup>b</sup>
1	( <i>RS</i> )- <b>2</b>	toluene/cyclohexane	Purified
2	( <i>R</i> )- <b>2</b>	CH <sub>2</sub> Cl <sub>2</sub> /cyclohexane	Purified
3	( <i>R</i> )- <b>2</b>	toluene/ <i>n</i> -hexane	Purified
4	( <i>RS</i> )- <b>3</b>	CHCl <sub>3</sub> /EtOH	Not Purified
5	( <i>RS</i> )- <b>4</b>	CH <sub>2</sub> Cl <sub>2</sub> /EtOH	Not Purified

a) All solvents used in a 1:1 volumetric ratio; b) Purified or not purified from the presence of contaminating regioisomers.

**Optical microscope and X-ray structure analyses of single crystals.** Crystals of the compounds (grown under the conditions shown in Table 1) were inspected using a polarising optical microscope, checking for the birefringence that should characterise single crystals. The morphologies of the crystals evidenced marked differences depending on the degree of regioisomeric purity of the compounds (Fig. 3 and Supporting Information).

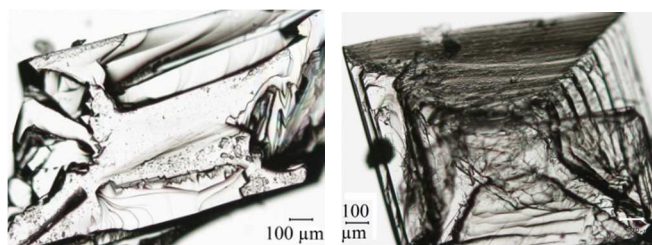


**Fig. 3** Morphology of crystals of **3**. The micrograph on the left shows crystals obtained after chemical functionalization from samples of **2** contaminated with regioisomers, while the formation of much higher quality single crystals (on the right) were obtained after chemical functionalization starting from regioisomerically pure **2**.

It is interesting to note that, although large amount of literature references can be found for the preparation of **2** (racemic or enantiopure), the X-ray structure of this compound has not been reported before. In previous papers, x-ray structures had been reported, but it was crystallised with the addition of secondary molecules, helping the crystal formation that are incorporated in the asymmetric unit.<sup>12</sup>

The crystal structure of (*R*)-**2** shows the characteristic quasi-perpendicular disposition of the naphthyl rings (Fig.4), where the torsion angle at the positions bearing the oxygen atoms is -105°. The compound crystallises in the *P*2<sub>1</sub>2<sub>1</sub>2<sub>1</sub> space group with four identical molecules in the unit cell. The Flack parameter for this chiral compound is in accord with the

expected value. The molecules pack forming what can be described as interdigitated layers. Within the layers O-H...O hydrogen bonds between hydroxyl groups in adjacent molecules (H...O distance 2.13 Å, O-H...O angle 164°) and C-H...π interactions between molecules (H...C distance 2.88 Å, C-H-C angle 123°) are present (see Table in ESI for details). Between the sheets, interactions between bromine atoms and protons on neighbouring molecules are apparent (C-Br...H-O, H...Br distance of 2.74 Å and C-Br...H-C, H...Br distance of 3.02 Å).

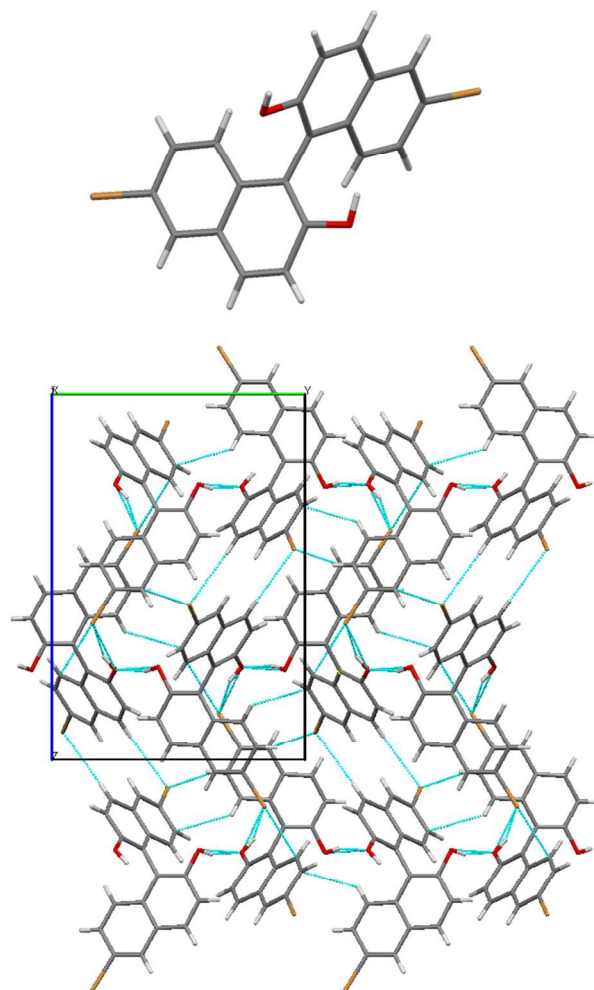


**Fig. 4** Views of the crystal structure of (*R*)-**2**. An image of the molecule (top) and its packing (below) seen along the *a* axis with short contacts indicated by light blue dotted lines.

The crystal structure of (*RS*)-**2** shows a similar quasi-perpendicular disposition of the naphthyl rings to the enantiopure compound, where the torsion angle at the positions bearing the oxygen atoms is somewhat lower ( $\pm 85^\circ$ ). The material is a true racemic compound in which the enantiomers are located at well defined position in the crystal lattice. The space group is *P*2<sub>1</sub>/*n*. The structure is formed by homochiral tapes in which the molecules are joined through hydrogen bonds (Fig. 5, see Table in ESI for details), where consecutive



molecules in the tape are joined through an O-H $\cdots$ O interaction between hydroxyl groups (H $\cdots$ O distance 2.15 Å, O-H $\cdots$ O angle 142°) and O-H $\cdots$  $\pi$  interactions (H $\cdots$ C distances 2.70 and 2.82 Å). These homochiral tapes pack into racemic sheets where there is an alternation of the chirality in each tape that comprises the layer (Fig. 6). The sheets are formed thanks to short contacts between bromine atoms and hydrogen atoms (C-Br $\cdots$ H-C, H $\cdots$ Br distance of 3.05 Å Br2—H5) and between a hydrogen and carbon atom in the naphthyl system within the tape (consistent with a C-H $\cdots$  $\pi$  interaction, H $\cdots$ C distance 2.96 Å, C-H-C angle 158°, H18—C3A). These corrugated heterochiral sheets stack on top of one another in the crystal with a short C-Br $\cdots$ H-C interaction (distance of 2.90 Å, Br2—H8), and a  $\pi$ - $\pi$ -interaction of 3.59 Å (C15—C17A).

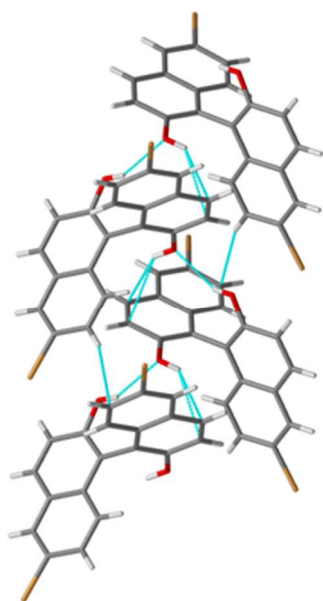


Fig. 5 View of the homochiral tapes in the crystal structure of (RS)-2. Short contacts indicated by light blue dotted lines.

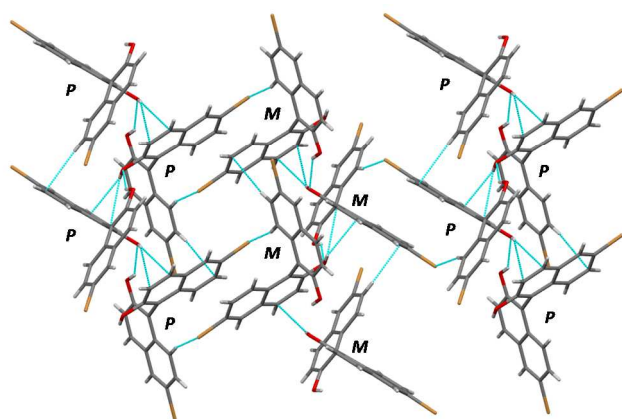


Fig. 6 View of the heterochiral sheets in the crystal structure of (RS)-2. Short contacts indicated by light blue dotted lines. *P* and *M* correspond to the helical chirality of each molecule.

Enantiopure (*R*)-3 – in which the oxygen atoms attached to the naphthyl moieties are now of the ether type – stacks in its crystals forming dimers (Fig. 7). These two molecules have distinct conformations (the torsion angles between the naphthyl

rings are -72° and -101°) and there are two non-equivalent dimers. In one dimer the distance between  $\pi$  systems is 3.34 Å at its smallest (there is a slight splaying) and this interaction is accompanied by a C-H $\cdots$  $\pi$  interaction (H $\cdots$ C distance 2.80 Å, C-H-C angle 140°) from one of the methylene units in the chain attached to the binaphthyl moiety. In the other the distance between  $\pi$  systems is 3.39 Å at its smallest (there is a slight splaying) and this interaction is accompanied by a C-H $\cdots$  $\pi$  interaction (H $\cdots$ C distance 2.89 Å, C-H-C angle 161°) from one of the methylene units in the chain attached to the binaphthyl moiety. There are also C-H $\cdots$ O interactions present in both dimers (indicated in Fig. 7). These two dimers alternate in a chain that runs along the *b* axis of the crystal. Between these chains there are interactions between bromine and hydrogen atoms seen in the other compounds in this series.

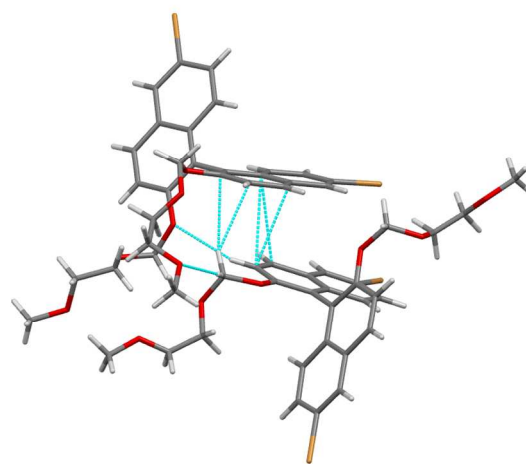
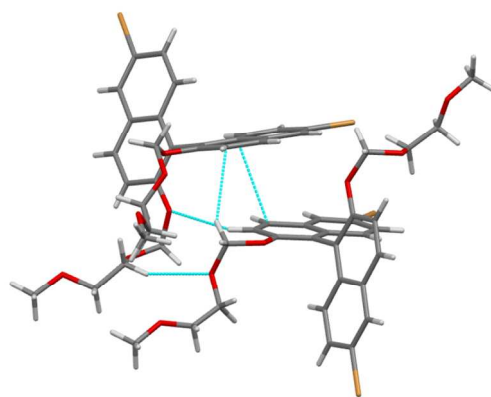
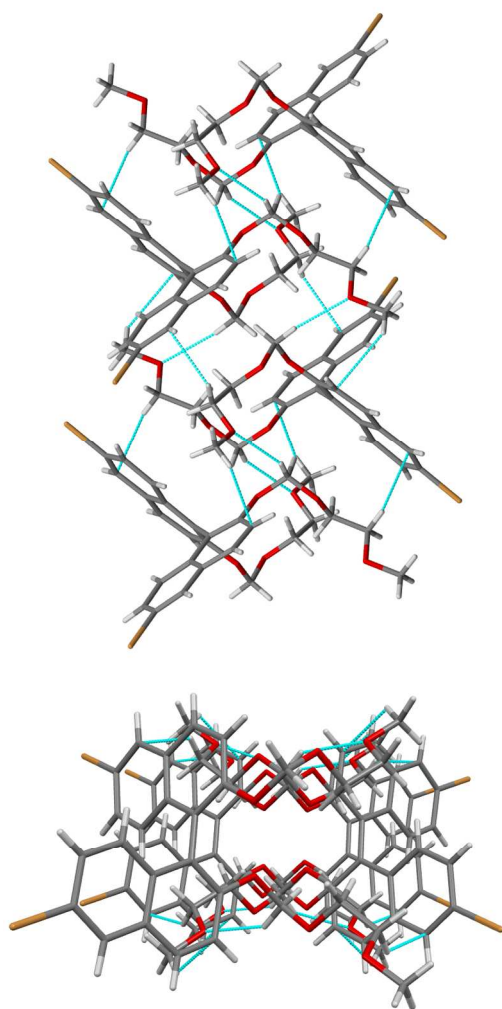


Fig. 7 Views of the non-equivalent dimers in the crystal structure of (*R*)-3. Short contacts indicated by light blue dotted lines.



**Fig. 8** Views of the heterochiral chains in the crystal structure of (RS)-**3**. Top side-on and below a perspective view along the chains. Short contacts indicated by light blue dotted lines.

In the racemic modification of **3**, a true racemic compound is formed with a structure pertaining to the *P*-1 space group and in which chains of alternating chirality zig-zag down the *a* axis (Fig. 8). There are no significant interactions between  $\pi$  systems (in contrast to the enantiopure compound), instead the alternating *R* and *S* molecules are connected through a series of C-H $\cdots$ O and C-H $\cdots$  $\pi$  interactions. Like chirality molecules are located “on top” of one another with the enantiomer making a non-covalent link between them through the bridging achiral side-groups.

The racemic form of **4**, in common with **3**, is a racemic compound where rows of one enantiomer line up next to a row of the other and where weak hydrogen bonds unite the molecules (Fig. 9). Again, the space group is *P*-1, but in this case the molecules form a sheet in the *ab* plane. As for **3**, the achiral side-groups link enantiomers non-covalently and like enantiomers are atop one another presumably as propellers stack on top of one another: Although there is no direct contact between them it is clear that one enantiomer in this position

would not fit in a dense packing arrangement. It is therefore the interactions between these “stacks” that lead to the racemic compound. The shortest non-covalent bonds involve the carbonyl group that forms a trifurcated hydrogen bond with three C-H groups (H $\cdots$ O distances 2.43, 2.52 and 2.67 Å, C-H $\cdots$ C angles 174°, 157° and 134°, respectively) and the head-to-tail stacked carbonyl groups along the *a*-axis (C $\cdots$ O distance 3.05 Å, C-O-C angles 102°).

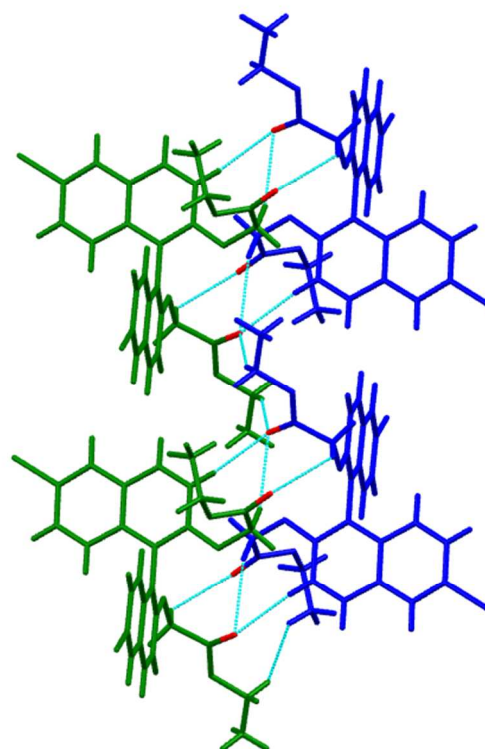


**Fig. 9** View of the heterochiral sheet in the crystal structure of (RS)-**4**. The chains shown run along the *b* axis, short contacts between carbonyl oxygen atoms (in red) and hydrogen atoms are indicated by light blue dotted lines. Enantiomers are shown in green and blue, respectively

**Disorder of the bromine atoms in the structures.** It was during the study of the crystals of (RS)-**4** that the presence of regioisomers was discerned: The bromine atoms should formally be located at the 6 and 6' positions assuming a totally selective reaction, but in the solid state structure they were also evident (because of electron density in the diffraction data) in low proportions at the 5 or 5' positions (but not at both in the same molecule apparently). This occupational disorder also led to a positional disorder caused by the proximity of bromine atoms in the “wrong” positions in neighbouring molecules. This solid solution can be interpreted through the presence of four molecules, which are shown in Figure 10. They are the main and desired 6,6' isomer (84%, top in Figure 10), a molecule resulting in disorder because of bromination at the Br2A position (6%, next to top in Figure 10), an isomer resulting in disorder because of bromination at Br1A (4%, next

to bottom in Figure 10) and a form of the desired isomer (6%, bottom in Figure 10) with a more twisted conformation than the major component, a distortion that arises because of an interaction between Br2A of one molecule with Br1 of a neighbouring molecule in the cell.

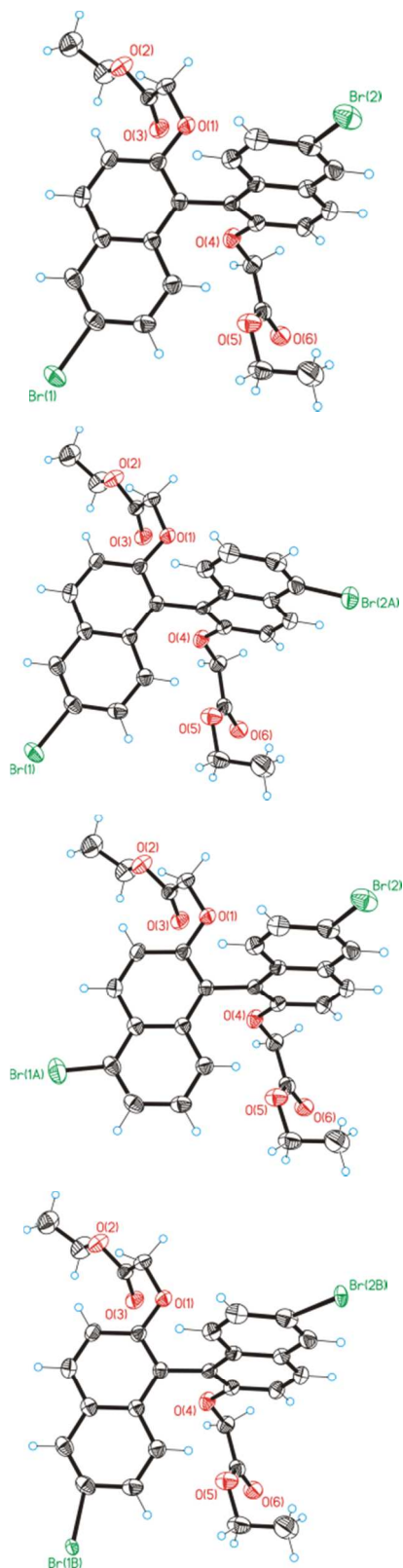


**Fig. 10** Four molecules present in the solid solution formed by (*RS*)-**4** and impurities in it. The top image shows the main and desired compound, below it different isomers of the compound with bromine atoms at 5 and 6 positions, and bottom the desired isomer with positional disorder caused by the proximity of bromine atoms from the impurities.

In detail, the major bromine positions Br1 at C6 with occupancy of 0.90 and Br2 at C17 with 0.88 come from the main compound. Br1A at C5 with occupancy of 0.04 and Br2A at C16 with 0.06 come from the impurity of the isomeric compound. Within the cell, the Br2A position has a distance of 2.62 (and 2.67) Å to Br1 (and Br1A) of a neighbouring molecule. This distance is too close for comfort and the neighbouring molecule will be twisted. Therefore positional disorder around Br1 and Br2 (twisting) occurs by the additional position Br1B and Br2B, each occupied with 0.06. The Br1A position also shows a short distance to the position Br2B with 2.74 Å, but because of the 4% and 6% distribution of these positions this plays no further role. Because only 6% of neighbouring molecules are twisted, this disorder could not be observed at the carbon atoms (low movement and anisotropic displacement parameters appear normal).

This disorder and the result that is a solid solution makes the purification of the compound at this stage of the synthesis of derivatives of these compounds unfeasible by crystallization.

## Conclusions

The electrophilic aromatic bromination reaction of BINOL leads predominantly to reaction at the 6,6' positions but alternatively at the 5,5' positions. The presence of regioisomeric compounds was revealed definitively by single crystal X-ray analysis of the solids formed during crystal growth of the crude products after subsequent reactions that showed the presence of solid solutions, a fact that was possible because bromine – being a heavy atom – is easily located by crystallography. Thus, the purification of the 6,6'-dibromo-1,1'-binaphthalene-2,2'-diol is essential before further reactions are performed.

In all the racemates studied here, the racemic compound is the favoured form in the crystal. While homochiral associations can be picked out in the crystals – largely because of steric interactions between non-like enantiomers that leads to enantiophobicity<sup>13</sup> at the stack level – the columns or layers come together in alternate fashion. The enantiopure compounds pack thanks to relatively weak interactions on the whole, and these are apparently overcome to make the racemic compounds. The structures provide important information for the design of new binaphthyl compounds that are synthetically easily accessed and that may lead to interesting properties as chiral materials.

## Experimental Section

**Synthesis.** The starting material (*RS*)-**1** (racemic) and (*R*)-**1** ((+)-BINOL) were purchased by Sigma-Aldrich with a purity of 99%, and used as received. All other commercially-available compounds and reactants were used as purchased. THF and



$\text{CH}_2\text{Cl}_2$  were dried and distilled before use. Compounds (*R*)- or (*RS*)-**2**,<sup>9</sup> (*R*)- or (*RS*)-**3**,<sup>10</sup> were prepared following published procedures. Thin layer chromatography was performed on silica gel on aluminium plates, and flash chromatography was performed on silica gel, pore size 60 Å.  $^1\text{H}$ -NMR spectra were recorded on 300 MHz and 400 MHz spectrometers in  $\text{CDCl}_3$  solutions with the solvent residual protons or TMS as internal standards. IR spectra were recorded using a Perkin Elmer spectrometer with attenuated total reflection attachment. Mass spectra were recorded using a Bruker MALDI instrument in reflectron mode. Circular Dichroism spectroscopy (Fig. S9) was performed in 1 cm quartz cells recording the spectra at 25 °C using a JASCO spectropolarimeter at a scanning speed of 50 nm min<sup>-1</sup> and pure solvent spectra were subtracted.

**Compound (*R*)-4.**<sup>11</sup> A suspension of (*R*)-**2** (3.04 g, 6.85 mmol, 1 eq) and  $\text{Cs}_2\text{CO}_3$  (15.81 g, 48.5 mmol, 7 eq) in DMF (100 mL) was stirred for 30 min at room temperature and then ethyl bromoacetate (3 mL, 27.1 mmol, 4 eq) was added at once. The pale yellow solution was stirred overnight.  $\text{H}_2\text{O}$  (120 mL) was added, and the homogeneous solution was extracted with  $\text{Et}_2\text{O}$  (3 x 250 mL), and then the organic phase dried ( $\text{MgSO}_4$ ). Purification by flash chromatography ( $\text{SiO}_2$ ; hexanes–ethyl acetate, from 75/25 to 60/40) yielded (*R*)-**4** as a yellowish solid in quantitative yield. IR (ATR, cm<sup>-1</sup>) 2980, 1730, 1580, 1490, 1190.  $^1\text{H}$  NMR ( $\text{CDCl}_3$ , 300 MHz, 25 °C)  $\delta$  = 8.03 (d, 2H; binaphthyl), 7.86 (d, 2H; binaphthyl), 7.35–7.30 (m, 4H; binaphthyl), 7.06 (d, 2H; binaphthyl), 4.56 (dd, 4H;  $-\text{OCH}_2\text{COO}-$ ), 4.13 (q, 4H;  $-\text{COOCH}_2\text{CH}_3$ ), 1.18 (t, 6H;  $-\text{COOCH}_2\text{CH}_3$ ).  $^{13}\text{C}$  NMR ( $\text{CDCl}_3$ , 75 MHz, 25 °C)  $\delta$  = 168.9 ( $\text{C}_{\text{quat}}$ ), 153.8 ( $\text{C}_{\text{quat}}$ ), 132.3 ( $\text{C}_{\text{quat}}$ ), 130.7 ( $\text{C}_{\text{quat}}$ ), 129.9 (CH), 129.8 (CH), 128.9 (CH), 127.3 (CH), 119.7 ( $\text{C}_{\text{quat}}$ ), 118.0 ( $\text{C}_{\text{quat}}$ ), 116.0 (CH), 66.7 ( $\text{CH}_2$ ), 61.1 ( $\text{CH}_2$ ), 14.0 ( $\text{CH}_3$ ).

**Crystallization procedure.** All the crystallization processes were obtained following the same procedure: first of all, the products (**2**, **3**, **4**) both in the enantiomeric (*R*) and racemic (*RS*) forms were isolated after the work up and dried under vacuum. Then, in small (3 mL) vials, a few milligrams (less than 10 mg) of the compounds were dissolved in 1 mL of a good dissolving solvent, such as the halogenated ones or toluene; 1 mL of a second solvent, in which the compounds were not soluble, was added at the vial very slowly, leaving the two solvents to equilibrate at the contact surface. The vials were left open and nice crystals were obtained after evaporation of part of the solvent mixture. The remaining solvent was removed with a Pasteur pipette and the crystals were washed with a few drops of the non-solvent. No more steps were necessary and all the analysis were carried out on the crystals as they precipitated.

**Optical imaging.** Optical micrographs were obtained using an Olympus BX51 microscope in transmission mode, using the variable angle polarising filters at 90° for the crossed polarised images, and were recorded using a DP20 digital camera.

## Acknowledgements

MA wishes to acknowledge an Erasmus Placement Fellowship from the University of Pavia supporting his stay in Barcelona. DP acknowledges support from MIUR (Programs of National Relevant Interest PRIN grant 2009-A5Y3N9), and, in part, from CARIPLO Foundation (2007–2009) and INSTM-Regione Lombardia (2010–2012 and 2013–2015). DBA thanks the MINECO, Spain, project CTQ2010-16339, and the DGR, Catalonia, project 2009 SGR 158.

## Notes and references

<sup>a</sup> Institut de Ciència de Materials de Barcelona (ICMAB-CSIC), Campus Universitari de Bellaterra, 08193 Cerdanyola del Vallès, Catalonia - Spain, Fax: (+34) 93-5805729

<sup>b</sup> Department of Chemistry and INSTM Research Unit, University of Pavia, Viale Taramelli, 10 - 27100 - Pavia - Italy.

<sup>c</sup> Institut für Anorganische Chemie, Innrain 80/82, A-6020 Innsbruck, Austria

† Electronic Supplementary Information (ESI) available: additional NMR spectra, IR spectra of selected compounds, optical microscope images of crystals, CD spectra, tables containing hydrogen bond data. See DOI: 10.1039/b000000x/

†† A literature search revealed several published experimental procedures for the preparation of (*R*)-**2** or (*RS*)-**2** from **1**; all of them report very similar reaction protocols (ref. 9): use of molecular bromine as the electrophile, dry  $\text{CH}_2\text{Cl}_2$  as the solvent, low temperatures (-80 °C to -20 °C), and inert atmosphere. None of these papers mention regioisomeric impurities.

‡ Crystal data for (*R*)-**2**, (*RS*)-**2**, (*R*)-**3**, (*RS*)-**3** and (*RS*)-**4**:

(*R*)-**2**:  $\text{C}_{20}\text{H}_{12}\text{Br}_2\text{O}_2$ ,  $M_r$  = 444.12, orthorhombic,  $P2_12_12_1$ ,  $a$  = 8.2300(2) Å,  $b$  = 11.8142(3) Å,  $c$  = 17.1253(3) Å,  $V$  = 1665.11(7) Å<sup>3</sup>,  $Z$  = 4,  $T$  = 233 K, 10638 reflections collected, 3263 independent reflections with  $R_{\text{int}}$  = 0.055.  $R$  ( $wR$ ) = 0.0288 (0.0676) for 2989 reflections with  $I > 2\sigma(I)$ ,  $R$  ( $wR$ ) = 0.0342 (0.0699) for all data. Flack  $x$  = 0.04(1). CCDC 1007143.

(*RS*)-**2**:  $\text{C}_{20}\text{H}_{12}\text{Br}_2\text{O}_2$ ,  $M_r$  = 444.12, monoclinic,  $P2_1/n$ ,  $a$  = 9.9622(3) Å,  $b$  = 8.3317(2) Å,  $c$  = 19.9628(5) Å,  $\beta$  = 98.208(1)°,  $V$  = 1639.98(8) Å<sup>3</sup>,  $Z$  = 4,  $T$  = 233 K, 10154 reflections collected, 3215 independent reflections with  $R_{\text{int}}$  = 0.042.  $R$  ( $wR$ ) = 0.0304 (0.0724) for 2781 reflections with  $I > 2\sigma(I)$ ,  $R$  ( $wR$ ) = 0.0389 (0.0758) for all data. CCDC 1007145.

(*R*)-**3**:  $\text{C}_{28}\text{H}_{28}\text{Br}_2\text{O}_6$ ,  $M_r$  = 620.32, monoclinic,  $P2_1$ ,  $a$  = 9.0274(2) Å,  $b$  = 20.4427(4) Å,  $c$  = 14.5383(3) Å,  $\beta$  = 99.274(1)°,  $V$  = 2647.89(10) Å<sup>3</sup>,  $Z$  = 4,  $T$  = 233 K, 17115 reflections collected, 9297 independent reflections with  $R_{\text{int}}$  = 0.034.  $R$  ( $wR$ ) = 0.0420 (0.0962) for 7863 reflections with  $I > 2\sigma(I)$ ,  $R$  ( $wR$ ) = 0.0560 (0.1021) for all data. Flack  $x$  = 0.022(7). CCDC 1007144.

(*RS*)-**3**:  $\text{C}_{28}\text{H}_{28}\text{Br}_2\text{O}_6$ ,  $M_r$  = 620.32, triclinic,  $P-1$ ,  $a$  = 9.8523(3) Å,  $b$  = 10.1793(3) Å,  $c$  = 13.9220(3) Å,  $\alpha$  = 70.723(2)°,  $\beta$  = 89.926(2)°,  $\gamma$  = 82.549(2)°,  $V$  = 1305.53(6) Å<sup>3</sup>,  $Z$  = 2,  $T$  = 233 K, 7962 reflections collected, 4588 independent reflections with  $R_{\text{int}}$  = 0.029.  $R$  ( $wR$ ) = 0.0357 (0.0804) for 3713 reflections with  $I > 2\sigma(I)$ ,  $R$  ( $wR$ ) = 0.0499 (0.0851) for all data. CCDC 1007146.

(*RS*)-**4**:  $\text{C}_{28}\text{H}_{24}\text{Br}_2\text{O}_6$ ,  $M_r$  = 616.29, triclinic,  $P-1$ ,  $a$  = 8.8364(2) Å,  $b$  = 10.5814(3) Å,  $c$  = 14.7993(3) Å,  $\alpha$  = 108.781(1)°,  $\beta$  = 94.787(1)°,  $\gamma$  = 97.419(1)°,  $V$  = 1287.54(5) Å<sup>3</sup>,  $Z$  = 2,  $T$  = 233 K, 8475 reflections collected, 5044 independent reflections with  $R_{\text{int}}$  = 0.032.  $R$  ( $wR$ ) = 0.0359 (0.0815) for 4026 reflections with  $I > 2\sigma(I)$ ,  $R$  ( $wR$ ) = 0.0514 (0.0872) for all data. CCDC 1007147.



- 1 a) J. J. L. M. Cornelissen, A. E. Rowan, R. J. M. Nolte and N. A. J. M. Sommerdijk, *Chem. Rev.*, 2001, **101**, 4039–4070. b) L. Pérez-García and D.B. Amabilino, *Chem. Soc. Rev.*, 2002, **31**, 342–356. c) F. J. M. Hoebe, P. Jonkheijm, E.W. Meijer and A. P. H. J. Schenning, *Chem. Rev.*, 2005, **105**, 1491–1546. d) D. K. Smith, *Chem. Soc. Rev.*, 2009, **38**, 684–694. e) M. Yanga and N. A. Kotov, *J. Mater. Chem.*, 2011, **21**, 6775–6792. f) J. A. A. W. Elemans, I. De Cat, H. Xu and S. De Feyter, *Chem. Soc. Rev.*, 2009, **38**, 722–736. g) J. Kumaki, S. Sakurai and E. Yashima, *Chem. Soc. Rev.*, 2009, **38**, 737–746. h) J. W. Canary, *Chem. Soc. Rev.*, 2009, **38**, 747–756. i) C. Noguez and I. L. Garzón, *Chem. Soc. Rev.*, 2009, **38**, 757–771. j) F. Vera, J. L. Serrano and T. Sierra, *Chem. Soc. Rev.*, 2009, **38**, 781–796. k) J. Clayden, *Chem. Soc. Rev.*, 2009, **38**, 817–829. l) J. Crassous, *Chem. Soc. Rev.*, 2009, **38**, 830–84.
- 2 a) L. Pu, *Chem. Rev.*, 1998, **98**, 2405–2494. b) Y. Chen, S. Yekta and A. K. Yudin, *Chem. Rev.*, 2003, **103**, 3155–3211. c) P. Kocovsky, S. Vyskocyl and M. Smrcina, *Chem. Rev.*, 2003, **103**, 3213–3245. d) J. M. Brunel, *Chem. Rev.*, 2005, **105**, 857–898.
- 3 a) M. Shibasaki, M. Kanai, S. Matsunaga and N. Kumagai, *Acc. Chem. Res.*, 2009, **42**, 1117–1127. b) B. Maciá Ruiz, K. Geurts, M. A. Fernández-Ibáñez, B. ter Horst, A. J. Minnaard and B. L. Feringa, *Org. Lett.*, 2007, **9**, 5123–5126. c) E. F. Di Mauro and M. C. Kozlowski, *Org. Lett.*, 2001, **3**, 1641–1644. d) V. Rauniar and D. G. Hall, *Synthesis*, 2007, 3421–3426. e) A. Alexakis, F. Romanov-Michailidis, L. Guenee, *Angew. Chem. Int. Ed.*, 2013, **52**, 9266–9270. f) C. Coluccini, A. Castelluccio and D. Pasini, *J. Org. Chem.*, 2008, **73**, 4237–4240.
- 4 a) D. J. Cram, R. Helgeson, S. C. Peacock, L. J. Kaplan, L. A. Domeier, P. Moreau, K. Koga, J. M. Mayer, Y. Chao, M. G. Siegel, D. H. Hoffman and G. D. Y. Sogah, *J. Org. Chem.*, 1978, **43**, 1930–1946. b) A. S. Droz, U. Neidlein, S. Anderson, P. Seiler and F. Diederich, *Helv. Chim. Acta*, 2001, **84**, 2243–2289. c) A. Bähr, A. S. Droz, M. Püntener, U. Neidlein, S. Anderson, P. Seiler and F. Diederich, *Helv. Chim. Acta*, 1998, **81**, 1931–1963. d) T. Kawase, T. Nakamura, K. Utsumi, K. Matsumoto, H. Kurata and M. Oda, *Chem. Asian J.*, 2008, **3**, 573–577. e) Z.-B. Li, J. Lin, H.-C. Zhang, M. Sabat, M. Hyacinth and L. Pu, *J. Org. Chem.*, 2004, **69**, 6284–6293. f) Z.-B. Li, J. Lin and L. Pu, *Angew. Chem. Int. Ed.*, 2005, **44**, 1690–1693. g) J. Heo and C. A. Mirkin, *Angew. Chem. Int. Ed.*, 2006, **45**, 941–944. h) A. Bencini, C. Coluccini, A. Garau, C. Giorgi, V. Lippolis, L. Messori, D. Pasini and S. Puccioni, *Chem. Commun.*, 2012, **48**, 10428–10430.
- 5 a) L. Izotova, B. Ibragimov, J. Ashurov, S. Talipov and E. Weber, *Cryst. Growth Des.*, 2006, **6**, 2523–2529. b) T. Tu, T. Maris, J. D. Wuest, *Cryst. Growth Des.*, 2008, **8**, 1541–1546. c) C. Coluccini, D. Dondi, M. Caricato, A. Taglietti, M. Boiocchi and D. Pasini, *Org. Biomol. Chem.*, 2010, **8**, 1640–1649. d) M. Boiocchi, M. Bonizzoni, A. Moletti, D. Pasini and A. Taglietti, *New J. Chem.*, 2007, **31**, 352–356. e) L. Q. Ma and W. B. Lin, *Angew. Chem. Int. Ed.*, 2009, **48**, 3637–3640. f) L. Ma, J. M. Falkowski, C. Abney and W. B. Lin, *Nature Chem.*, 2010, **2**, 838–846. g) M. E. Belowich, Y. Y. Botros, T. Gasa, J. F. Stoddart, C. Valente, E. Choi, C. J. Doonan, Q. Li and O. M. Yaghi, *Chem. Commun.*, 2010, **46**, 4911–4913.
- 6 A. Shokravi, A. Javadi and E. Abouzari-Lotf, *RSC Advances*, 2013, **3**, 6717–6746.
- 7 a) M. Caricato, N. J. Leza, K. Roy, D. Dondi, G. Gattuso, L. S. Shimizu, D. A. Vander Griend and D. Pasini, *Eur. J. Org. Chem.*, 2013, 6078–6083. b) M. Caricato, A. Olmo, C. Gargiulli, G. Gattuso and D. Pasini, *Tetrahedron*, 2012, **68**, 7861–7866. c) M. Caricato, C. Coluccini, D. Dondi, D. A. Vander Griend and D. Pasini, *Org. Biomol. Chem.*, 2010, **8**, 3272–3280. d) A. Moletti, C. Coluccini, D. Pasini and A. Taglietti, *Dalton Trans.*, 2007, **16**, 1588–1592.
- 8 a) D. Pasini and M. Ricci, *Curr. Org. Synth.*, 2007, **4**, 59–80. b) M. Caricato, A. K. Sharma, C. Coluccini and D. Pasini, *Nanoscale*, 2014, **6**, 7165–7174.
- 9 Selected examples: a) Y. Cui, O. R. Evans, W. B. Lin, H. L. Ngo and P. S. White, *Angew. Chem. Int. Ed.*, 2002, **41**, 1159–1162. b) K. H. Doetz and A. Minatti, *Tetrahedron Asym.*, 2005, **16**, 3256–3267. c) Z. An, W. Huang, H. Shi, N. Shi, J. Yin, Z. An, R. Chen and H. Jiang, *J. Polym. Sci. A. Polym. Chem.*, 2010, **48**, 3868–3879. d) L. Chen, C.-Q. Li and M. Shi, *J. Am. Chem. Soc.*, 2005, **127**, 3790–3800. e) G. Gao, J. Lan, X. Su, F. Yang, J. You and L. Yang, *Org. Biomol. Chem.*, 2011, **9**, 2618–2621. f) Y. Harada, K. Onitsuka, S. Takahashi and F. Takei, *Chem. Commun.*, 1998, 643–644. g) M. Rueping, E. Sugiono, A. Steck and T. Theissmann, *Adv. Synth. Catal.*, 2010, **352**, 281–287. h) K. Hattori and S. Miyano, *J. Am. Chem. Soc.*, 1998, **120**, 9086–9087. i) G. C. Clarkson, C. L. North, M. Wills, Y. Xu, G. Docherty and G. Woodward, *J. Org. Chem.*, 2005, **70**, 8079–8087. j) H. Ishitani, S. Kobayashi, H. Shimizu and Y. Yamashita, *J. Am. Chem. Soc.*, 2002, **124**, 3292–3302. m) X. Liu, P. Wang, P. Wang, Q. Yang, Y. Yang and X. Liu, *Chem. Asian J.*, 2010, **5**, 1232–1239.
- 10 A. Brethon, P. Hesemann, J. J. E. Moreau, L. Rejaud and M. W. C. Man, *J. Organomet. Chem.*, 2001, **627**, 239–248.
- 11 C. Coluccini, A. Mazzanti and D. Pasini, *Org. Biomol. Chem.*, 2010, **8**, 1807–1815.
- 12 Selected examples: a) Y. Imai, N. Tajima, T. Sato and R. Kuroda, *Org. Lett.*, 2006, **8**, 2941–2944; b) R. Kuroda, Y. Imai and T. Sato, *Chirality*, 2001, **13**, 588–594; c) T. Kinuta, N. Tajima, T. Sato, R. Kuroda, Y. Matsubara and Y. Imai, *J. Mol. Struct.*, 2010, **964**, 27–30.
- 13 L. Pérez-García and D.B. Amabilino, *Chem. Soc. Rev.*, 2007, **36**, 941–967.